Relativistic time dilation at L2

Jos de Bruijne
Astrophysics Missions Division (SCI–SA)
RSSD/ESTEC/ESA
Postbus 299
NL–2200 AG Noordwijk (ZH)
The Netherlands
Jos.de.Bruijne@rssd.esa.int

Technical Note GAIA–JdB–003 (revision 1)
March 6, 2003

Abstract GAIA will perform its observations from a quasi-periodic Lissajous-type orbit around L2, the second Lagrange point of the Sun/Earth–Moon system. The satellite will therefore (1) be in continuous motion w.r.t. the Solar system barycenter, and (2) be subject to/embedded in a continuously varying gravitational potential. As a result, the clock on board the satellite, which provides the time standard for the centroiding measurements, will experience a time-variable amount of special relativistic kinematic and general relativistic gravitational time dilation. This technical note addresses these issues, and indicates that allowance for both effects must be made. A detailed analysis of GAIA's clock accuracy and stability requirements is presented in GAIA–JdB–004.

1 Introduction

A moving clock G is known to tick slower than an identical clock at rest. This special relativistic effect, referred to as kinematic time dilation, is described by a Lorentz-type formula:

$$T = \frac{T_{\rm G}}{\sqrt{1 - v_{\rm G}^2 c^{-2}}} \approx T_{\rm G} \cdot \left(1 + \frac{1}{2} \cdot \left[\frac{v_{\rm G}^2}{c^2} \right]^1 + \frac{3}{8} \cdot \left[\frac{v_{\rm G}^2}{c^2} \right]^2 + \frac{5}{16} \cdot \left[\frac{v_{\rm G}^2}{c^2} \right]^3 + \ldots \right) , \tag{1}$$

where $T_{\rm G}$ is the proper time, i.e., the time measured in the rest frame of the clock, T is the corresponding time measured in the frame w.r.t. which the clock moves with velocity $v_{\rm G}$, and $c = 299\,792\,458$ m s^{-1} is the speed of light in vacuum.

In addition to special relativistic kinematic time dilation, a clock can experience general relativistic gravitational time dilation: a clock G in a gravitational field runs more slowly than an identical clock in the absence of gravitational forces. The corresponding time dilation relationship from general relativity is:

$$T = \frac{T_{\rm G}}{\sqrt{1 - 2U_{\rm G} c^{-2}}} \approx T_{\rm G} \cdot \left(1 + \frac{1}{2} \cdot \left[\frac{2U_{\rm G}}{c^2} \right]^1 + \frac{3}{8} \cdot \left[\frac{2U_{\rm G}}{c^2} \right]^2 + \frac{5}{16} \cdot \left[\frac{2U_{\rm G}}{c^2} \right]^3 + \ldots \right) , \tag{2}$$

where $T_{\rm G}$ is the time interval measured by clock G, T is the corresponding time interval measured by an identical clock far away from the gravitational field, $U_{\rm G} = GMr^{-1}$ is, apart from a minus sign, the Newtonian gravitational potential felt by clock G, M is the mass generating the potential $U_{\rm G}$, $G = 6.672\,59 \times 10^{-11}$ m^3 kg^{-1} s^{-2} is Newton's universal constant of gravitation, and r is the distance from clock G to the (center of the) mass. A well-known manifestation of gravitational time dilation is the Shapiro (1964) delay measured for interplanetary signal propagation.

In the case of (a clock on board) GAIA, both kinematic and gravitational time dilation play a role. The kinematic effect is to be accounted for by knowledge of the instantaneous satellite velocity w.r.t. the Solar

system barycenter, which will be obtained by means of satellite ranging and Doppler measurements. The gravitational effect is to be accounted for by means of a Solar system ephemeris, which will be used for the calculation of the instantaneous potential felt by the satellite.

2 Time scales and transformations

This section presents a concise review of time systems, time transformations, and related aspects (see also Figure 1). For more information, we refer the reader to Seidelmann (1992), Seidelmann & Fukushima (1992), ESA (1997), and Brumberg & Groten (2001). Familiarity with the material treated here is not strictly needed to follow the main theme of this Technical Note, and some readers may therefore want to go directly to §3.

2.1 TDB and TDT

As explained in §1, the rate of a clock depends on the gravitational potential and its motion with respect to other clocks. Thus, the time scale entering the equations of motion depends on the coordinate system to which the equations refer. Since 1984, *The Astronomical Almanac* referred to two such dynamical time scales: Terrestrial Dynamical Time (TDT) and Barycentric Dynamical Time (TDB).

TDT is the time reference for geocentric ephemerides; it is the time coordinate to go with space coordinates on the Earth's geoid (a particular equipotential surface in the gravity field of the Earth). TDT is tied to International Atomic Time (TAI) by a constant offset of +32.184 s (1 January 1977 $0^{\rm h}\ 0^{\rm m}\ 0^{\rm s}$ TAI = 1 January 1977 $0^{\rm h}\ 0^{\rm m}\ 32.184^{\rm s}$ TDT). This offset was chosen to give continuity with the previously used Ephemeris Time (ET). TAI is today's primary time standard: it is determined using the input of many ($\sim$230) atomic clocks around the world, each corrected for known environmental and relativistic effects. TAI is an Earth-based time since it is defined for a gravitational potential and inertial reference frame on the surface of the Earth (more precisely: the geoid). TAI is the standard for the SI second.

TDB is the time reference for ephemerides referred to the Solar system barycenter. TDB and TDT differ by small periodic relativistic correction terms to move the origin from the geoid to the Solar system barycenter (see §2.2.3 for details).

It is customary to specify Julian Date (JD) as SI seconds in TDT. By definition, the lengths of one Julian day, one Julian year, and one Julian century are 86 400 s, 365.25 d, and 36 525 yr, respectively. The Julian year is the time unit underlying the definition of proper motions in the Hipparcos and Tycho Catalogues (ESA 1997).

2.2 TCB and TCG

In 1991, the IAU adopted a set of resolutions introducing new time scales — within the framework of Einstein's general theory of relativity — which all have units of measurement consistent with the SI second as the unit of time (IAU Resolution A4, 1992; see `http://www.iers.org/`). The two new time scales corresponding with the time scales TDB and TDT are TCB and TCG; their offsets are defined such that:

$$\begin{array}{llcllll}
\text{1 January 1977} & 0^{\rm h}\ 0^{\rm m}\ 0^{\rm s} & \text{TAI} & = & \text{JD 2443144.5} & \text{TAI} & = \\
\text{1 January 1977} & 0^{\rm h}\ 0^{\rm m}\ 32.184^{\rm s} & \text{TDT} & = & \text{JD 2443144.500\,372\,5} & \text{TDT} & = \\
\text{1 January 1977} & 0^{\rm h}\ 0^{\rm m}\ 32.184^{\rm s} & \text{TCG} & = & \text{JD 2443144.500\,372\,5} & \text{TCG} & = \\
\text{1 January 1977} & 0^{\rm h}\ 0^{\rm m}\ 32.184^{\rm s} & \text{TCB} & = & \text{JD 2443144.500\,372\,5} & \text{TCB} & .
\end{array} \qquad (3)$$

In 2000, the IAU adopted a set of resolutions extending Resolution A4 (1992) to the first post-Newtonian level (e.g., Petit 2002).

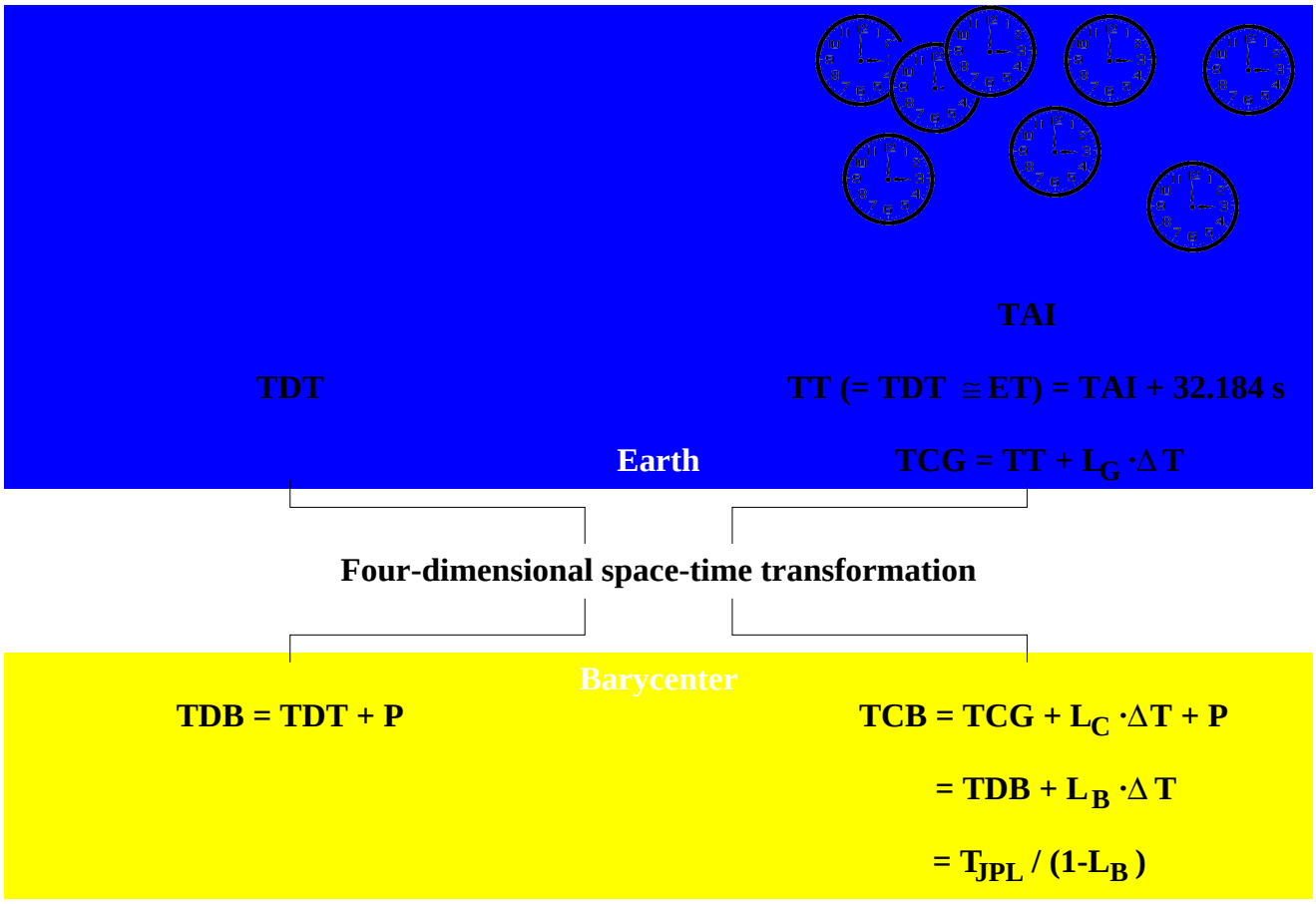

ΔT = (date in days - 1 January 1977 0^H) TAI · 86400 s
= (JD - 2443144.5003725) TT · 86400 s
P = sum of periodic terms with an average of zero
$T_{JPL} = T_{Eph}$ = Coordinate Time = CT = JPL ephemeris time
$L_B = L_G + L_C$

Figure 1: Graphical schematic summary of §2.

Barycentric Coordinate Time (TCB) is the time coordinate in the four-dimensional general relativistic barycentric reference system of the Solar system BCRS (Barycentric Celestial Reference System); loosely speaking, the three spatial coordinates of a four-vector in the BCRS can be thought of as materializing the International Celestial Reference System (ICRS). Similarly, Geocentric Coordinate Time (TCG) is the time coordinate in the four-dimensional general relativistic geocentric reference system GCRS (Geocentric Celestial Reference System); loosely speaking, the three spatial coordinates of a four-vector in the GCRS can be thought of as materializing the International Terrestrial Reference System (ITRS). The basic physical units of space-time in both BCRS and GCRS are the SI second for proper time and the SI meter for proper length (the SI meter is related to the SI second by means of c, the speed of light in vacuum).

The GCRS and related concepts such as TCG are practically useful when working in the immediate vicinity of the Earth, meaning up to altitudes of ∼50 000 km, thus including geostationary satellites. GAIA, however, will operate from L2, $\sim 1.5 \times 10^6$ km from Earth, which implies it is preferential to work directly in the BCRS whenever possible.

2.2.1 TCG versus TT

In 1991, the IAU recommended deleting the word Dynamical from Terrestrial Dynamical Time (TDT), leaving Terrestrial Time (TT). TT is the (theoretical) time reference for apparent geocentric ephemerides; it can be considered as equivalent to TDT.

By definition, TT differs from TCG, the time coordinate to go with space coordinates centered at the geocenter of the Earth, uniquely by a constant rate (e.g., Seidelmann 1992):

$$\mathrm{TCG} - \mathrm{TT} = L_\mathrm{G} \cdot (\mathrm{JD\ [TT]} - 2443144.500\,372\,5\ \mathrm{TT}) \cdot 86\,400, \tag{4}$$

where 86 400 is the number of SI seconds per Julian day, and $L_\mathrm{G} = 6.969\,290\,134 \times 10^{-10}$ is a defining constant (Brumberg & Groten 2001; Petit 2002).

Historically, L_G was defined in terms of $W_0 = 62\,636\,855.8\ \mathrm{m^2\ s^{-2}}$, the (gravitational plus spin) potential at the geoid, as $L_\mathrm{G} = c^{-2} W_0 = 6.969\,290\,112 \times 10^{-10}$ (Irwin & Fukushima 1999). This relationship, however, had the undesirable property that the definition of TT (equation 4) depended on the precise definition and realization of the geoid. In 2000, the IAU therefore adopted Resolution B1.9, characterizing L_G as a defining constant.

2.2.2 TCB versus TCG

In practice, TCB is defined in terms of TCG, which in its turn is defined in terms of TT (see equation 4): "TCB − TT = (TCB − TCG) + (TCG − TT)". Evaluation of TCB − TCG involves a four-dimensional transformation (e.g., equation 2.223-2 in Seidelmann 1992), which leads (in approximation) to:

$$\mathrm{TCB} - \mathrm{TCG} = L_\mathrm{C} \cdot (\mathrm{JD\ [TT]} - 2443144.500\,372\,5\ \mathrm{TT}) \cdot 86\,400 + c^{-2} \mathbf{v}_\mathrm{E} \cdot (\mathbf{x} - \mathbf{x}_\mathrm{E}) + P, \tag{5}$$

where L_C expresses the mean rate of the location-independent part of TCB − TCG, $\mathbf{x}$ is the barycentric position of the observer, $\mathbf{x}_\mathrm{E}$ and $\mathbf{v}_\mathrm{E}$ denote the barycentric position and velocity of the Earth's center of mass, and P represents the sum of periodic terms. These periodic corrections, which are collectively also referred to as the Einstein delay/term, consist of an annual sinusoidal term with amplitude ∼1.657 ms (due to the eccentricity of the Earth's orbit), planetary terms contributing up to ∼20 μs, and Lunar and diurnal terms contributing up to ∼2 μs (e.g., Seidelmann & Fukushima 1992).

Determination of the rate L_C involves a numerical integration of an Earth ephemeris; Fukushima & Irwin (1999), e.g., show that the JPL DE405/TE405 ephemerides result in $L_\mathrm{C} = 1.480\,826\,867\,41 \times 10^{-8}$ (including a post-Newtonian correction and a correction for the presence of (the 300 most massive) asteroids as a group; cf. §4.2 and Fukushima 1995).

2.2.3 TCB versus TDB

Barycentric Dynamical Time (TDB) is the same as TT (or TDT) except for — by definition periodic — relativistic corrections (due to the Earth's location and motion in the Solar system; "TDB = TT + P"). As a result, TCB and TDB differ only by a constant rate and offset:

$$\mathrm{TCB} - \mathrm{TDB} = L_\mathrm{B} \cdot (\mathrm{JD\ [TT]} - 2443144.500\,372\,5\ \mathrm{TT}) \cdot 86\,400, \tag{6}$$

where $L_\mathrm{B} = L_\mathrm{C} + L_\mathrm{G} - L_\mathrm{C} \cdot L_\mathrm{G}$; to sufficient approximation, one has $L_\mathrm{B} \approx L_\mathrm{C} + L_\mathrm{G}$. As the value of L_C depends on which Earth ephemeris is used, L_B is also ephemeris-dependent. Fukushima & Irwin (1999) derived $L_\mathrm{B} = 1.550\,519\,767\,49 \times 10^{-8}$ for the latest JPL ephemerides DE405/TE405.

Equation (6) implies that TCB diverges from TDB, or from TT, by $365.25 \cdot 24 \cdot 3600 \cdot 1.550\,519\,767\,49 \times 10^{-8} = 0.49\ldots\ \mathrm{s\ yr^{-1}}$. For example, at epoch J2000.0 (i.e., JD 2451545.0 TDB), TCB differed from TDB by 11.25 . . . s (see also Seidelmann & Fukushima 1992).

3 The relativistic time-dilation integral

The observational data of GAIA, i.e., the centroiding measurements, are parameterized by the proper time of the clock on board the satellite. It is currently recommended that the final GAIA catalogue, containing, among others, positions, parallaxes, and proper motions of the sources relative to the BCRS is parameterized by TCB (see Klioner 2002).

GAIA's clock will run at a different rate from TCB (see, e.g., equations 1–2; TCB will from here on also be denoted by the symbol T). In the Newtonian weak-field approximation[1] of general relativity, neglecting contributions of order c^{-4} and higher in the N-body metric tensor that describes the Solar system, TCB and the clock's proper time $T_{\rm G}$ are related through (e.g., Standish 1998a):

$$\frac{{\rm d}\,T_{\rm G}}{{\rm d}\,T} = 1 - c^{-2}\cdot\left(U_{\rm G} + \frac{v_{\rm G}^2}{2}\right), \tag{7}$$

where $U_{\rm G}$ is, apart from a minus sign, the Newtonian gravitational potential experienced by GAIA as a result of the masses of all bodies in the Solar system, and $v_{\rm G} = |\mathbf{v}_{\rm G}|$ is GAIA's barycentric velocity. Thomas (1975) claims that this formula contains all terms that lead to clock rate corrections ${\rm d}\,T_{\rm G}/{\rm d}\,T$ greater than 10^{-15} (cf. Petit 2002). Thomas (1975) also claims that, under the weak-field assumptions, it is justified to treat the space coordinates of general relativistic four-vectors in, e.g., the BCRS or GCRS as (Newtonian) three-dimensional vectors.

If $T_{\rm G}$ and T in equation (7) are measured in the same inherent units (e.g., SI seconds), we have:

$$T_{\rm G} - T = -\int_{T_0}^{T} c^{-2}\cdot\left(U_{\rm G} + \frac{v_{\rm G}^2}{2}\right)\,{\rm d}t, \tag{8}$$

where it is assumed that the two times are synchronized at T_0 so that $T_{\rm G} = T$ at T_0. The integral in equation (8) is generally referred to as the relativistic time-dilation integral. If, however, $T_{\rm G}$ and T are measured in different units, which is physically possible, equation (8) generalizes to (Standish 1998a):

$$T_{\rm G} - T = (K-1)\cdot(T - T_0) - K\cdot\int_{T_0}^{T} c^{-2}\cdot\left(U_{\rm G} + \frac{v_{\rm G}^2}{2}\right)\,{\rm d}t, \tag{9}$$

where K is a constant, and where it is again assumed that the two times are synchronized at T_0. Equation (9) reduces to equation (8) for $K = 1$.

3.1 TCB versus JPL ephemeris time CT

The independent variable, or time scale, of the fundamental general relativistic equations of motion governing the bodies of the Solar system (and as such the independent variable underlying the JPL planetary and Lunar ephemerides) is coordinate time (CT[2]). It can be shown that CT (which will hereafter also be denoted by the symbol $T_{\rm JPL}$) is physically and mathematically equivalent to the IAU definition of TCB (i.e., T), differing by only (an offset and) a constant rate (Fukushima 1995; Standish 1998a; Brumberg & Groten 2001):

$$T_{\rm JPL} = (1 - L_{\rm B})T, \tag{10}$$

[1] See Fukushima (1995; his §5) and Petit (2002; his equation 6) for discussions of post-Newtonian corrections and see Klioner (2002; his §4) for the relativistic consequences of the multipole structure of gravitating bodies and the gravitational field produced by their rotational motion.

[2] In the past, this time has erroneously been referred to (e.g., in JPL documentation and programs) first as Ephemeris Time (ET) and later (from 1976) as Barycentric Dynamical Time (TDB). See Standish (1998a) for details. In the literature, CT is sometimes referred to as $T_{\rm Eph}$, which is not to be confused with the obsolete Ephemeris Time (ET). We denote CT by $T_{\rm JPL}$.

where the constant $L_B = 1.550\,519\,767\,49 \times 10^{-8}$ for the latest JPL ephemerides DE405/TE405 (Fukushima & Irwin 1999). Equation (10) implies, given equation (6), that JPL's ephemeris time CT agrees in the long term with TT (see also Standish 1998a). Equation (10) also implies that TCB diverges from JPL's ephemeris time CT by $0.49\ldots$ s yr^{-1}. Note that equation (10) links to equation (9) for $K = (1 - L_B)^{-1}$.

Spatial coordinates x_{JPL} and masses M_{JPL} used in JPL ephemerides scale similarly as time:

$$x_{JPL} = (1 - L_B)x; \quad (11)$$

$$(GM)_{JPL} = (1 - L_B)GM, \quad (12)$$

where x and GM denote coordinates and masses in a TCB-based system (i.e., BCRS). Scaling relations (10)–(12) guarantee the invariance of the velocity of light c and the equations of motions of Solar system bodies under transformation from TCB to CT and vice versa. As a result of these relations, the values of some astronomical constants (e.g., the astronomical unit expressed in units of m and gravitational constants GM expressed in units of m^3 s^{-2}) depend on the adopted time system (cf. Table 2 in Seidelmann & Fukushima 1992 and Huang et al. 1995).

4 GAIA

In order to evaluate $T_G - T$ as a function of time, we need to evaluate the relativistic time-dilation integral (equation 8). We thus need $U_G = U_G(\mathbf{x}, t)$ and $\mathbf{x}_G = \mathbf{x}_G(t)$ (with $\mathbf{v}_G(t) = \mathrm{d}\,\mathbf{x}_G(t)/\mathrm{d}\,t$), i.e., the spatial and temporal dependence of the Solar system's potential to which GAIA will be subject/in which GAIA will be immersed during its operational life, and the barycentric orbit of the satellite. In the above, $\mathbf{x}$ and $\mathbf{v}$ denote three-dimensional coordinate and velocity vectors in the BCRS reference system, and t denotes TCB. Similarly, the integration variable t in the relativistic time-dilation integral (equation 8) is TCB; following Fukushima (1995) and Irwin & Fukushima (1999), we interpret t as CT (or T_{JPL}) instead of TCB (or T), thereby introducing a negligible error.

4.1 Kinematic time dilation for GAIA

During its operational life, GAIA's barycentric orbit $\mathbf{x}_G(t)$, and thus its barycentric velocity $\mathbf{v}_G(t)$, will be determined to high precision by satellite ranging and Doppler measurements (Pellón Bailón 2002; see also the discussion later in this section). In this investigation, we are merely interested in a simple yet realistic, and preferably analytic, prescription for the orbit of GAIA, e.g., relative to L2. Mignard (2002; his equation 87) provides such a description, which will be used here (see Appendix A and Figures 6–7 for details). GAIA's orbit w.r.t. the Solar system barycenter, $\mathbf{x}_G(t)$, is then simply obtained by vector-wise addition of the orbit of L2 w.r.t. the Solar system barycenter (available from the JPL DE405 ephemerides — see equation 14 in Appendix B) and GAIA's orbit w.r.t. L2.

Figure 2 shows the time evolution of that part of the integrand of the relativistic time-dilation integral that corresponds to kinematic time dilation, i.e., $c^{-2}v_G^2(t)/2$, split into the motion of L2 w.r.t. the Solar system barycenter ($v \sim 30$ km s^{-1}) and the motion of GAIA w.r.t. L2 ($v \sim 40$ m s^{-1}; cf. Figure 10 in Mignard 2002). We conclude from Figure 2 that, even for a clock stability of 6×10^{-13} over 6 h (i.e., 1.5×10^{-12} over 1 h; see §4.3 and GAIA–JdB–004), GAIA's orbital motion around L2 introduces a negligible effect in the kinematic part of the relativistic time-dilation integral.

The conclusion that GAIA's orbital motion around L2 introduces a negligible effect in the kinematic part of the relativistic time-dilation integral does not imply that accurate velocity determinations of the spacecraft will not be required. GAIA's aim is to obtain absolute astrometry at the level of $\delta \sim 1$ μas $\sim 5 \times 10^{-12}$ rad. This implies that the velocity of the satellite w.r.t. the Solar system barycenter needs to be known to a precision of order $c \cdot \delta \sim 1.5$ mm s^{-1} in order to be able to correct the apparent positions of objects observed by GAIA for stellar aberration (cf. Mignard

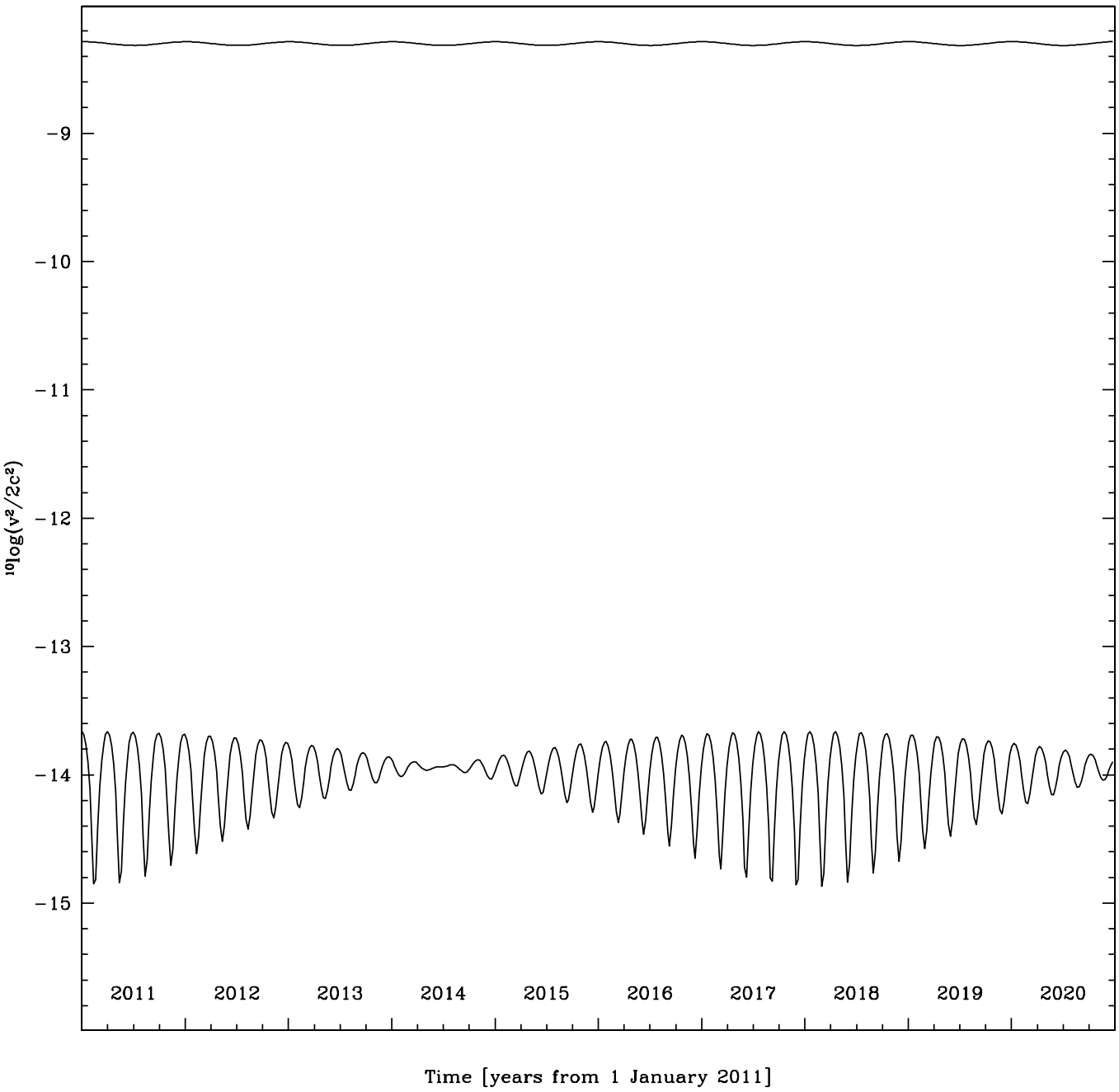

Figure 2: The contribution to $c^{-2}v_{\rm G}^2(t)/2$ of (1; upper curve) the velocity of L2 w.r.t. the Solar system barycenter ($v \sim 30$ km s^{-1} $\longrightarrow$ $c^{-2}v^2/2 \sim 5 \times 10^{-9}$) and (2; lower curve) GAIA's motion around L2 ($v \sim 40$ m s^{-1} $\longrightarrow$ $c^{-2}v^2/2 \sim 1 \times 10^{-14}$; see §4.1 for details). The figure covers a 10-year interval starting 1 January 2011 and is sampled at 7-day time steps. The velocity of GAIA w.r.t. L2 has been inferred by means of (analytic) differentiation of equation (13).

1998; in fact, stellar aberration will need to be accounted for up to order v^2/c^2).
Although stringent, the abovementioned velocity requirement of $\sim$1.5 mm s^{-1} is within reach. In practice, GAIA's barycentric orbit should be decomposed into (1) the Solar system barycenter–geocenter vector and (2) the geocenter–satellite vector. Around 2010, velocity errors related to the first component (the Earth ephemeris) are estimated to be $\sim$0.2 mm s^{-1} (see §5.4 and Table 5.3 in the GAIA Concept and Technology Study Report). Velocity errors related to the second component (Doppler measurement errors) are currently estimated to be $\sim$2–6 mm s^{-1} for a realistic mission and ground segment scenario (see Pellón Bailón 2002).

4.2 Gravitational time dilation for GAIA

JPL's DE405 ephemerides (Standish 1998b; see Appendix B for details) can be used to retrieve the locations of, e.g., the Sun, the planets, the Moon, asteroids, and L2, e.g., relative to the Solar system barycenter, as a function of CT (i.e., $T_{\rm JPL}$). This means that $U_{\rm G}(\mathbf{x},t)$ is readily available.

In order to investigate (at an order-of-magnitude level) which bodies in the Solar system contribute to gravitational time dilation at/near GAIA's observing location L2, we determined the first-order Taylor series expansion coefficient of equation (2), i.e., $U_{\rm G}c^{-2} = GMr^{-1}c^{-2}$, for the Sun, the Earth, the Moon, the planets and a number of their most massive moons (such as Io, Titan, and Ganymede), and the most massive of the "three big asteroids", Ceres (we thus neither consider the effects of tidal potentials of the Earth, the Moon, or the Sun nor the effects of the non-spherical shapes of the potentials of these bodies). Physical data of these bodies (notably orbital semi-major axes a and masses M) were taken from Table 1 in GAIA–JdB–001. For the distance r from the bodies to L2, we considered the extreme cases $r = |a - a_{\rm L2}|$ (providing a maximum value of $U_{\rm G}c^{-2}$) and $r = |a + a_{\rm L2}|$ (providing a minimum value of $U_{\rm G}c^{-2}$), where $a_{\rm L2} \approx 1.010\,078\,240\,44$ AU (see Appendix B for details).

Table 1 shows the results of this exercise, from which we conclude the following:

- the Sun provides, by far, the dominant effect of gravitational time dilation at L2 ($U_{\rm G}c^{-2} \sim 10^{-8}$);
- all planets and the Moon contribute to gravitational time dilation at L2 at the level of 10^{-15} or larger, with the exception of Pluto;
- the four Galilean moons of Jupiter as well as Titan contribute at the level of $\sim 10^{-16}$ or smaller;
- the most massive asteroid (Ceres) contributes at the level of $\sim 10^{-17.5}$.

Contributions due to individual asteroids can also be considered more generally. Let us assume asteroids are spherical bodies with a mean density $\rho_{\rm dens} = 3$ g cm^{-3}. Let us parameterize their sizes by the relationship $R_\alpha = 50 \times 10^\alpha$ m, where the range $\alpha = 0, \ldots, 4$ translates to the radius interval $R_{\alpha=0} = 50$ m to $R_{\alpha=4} = 500$ km (note that $R = 466$ km for Ceres, the largest asteroid). The minimum distance $r_{\rm min}$ at which an asteroid has to pass by an observer in order to generate a gravitational time dilation of order $10^{-\beta}$ is given by $r_{\rm min} = GMc^{-2}10^{+\beta} = 7.8 \times 10^{-30+\beta+3\alpha}$ AU, where $M = \frac{4}{3}\pi\rho_{\rm dens}R_\alpha^3$ is the mass of the asteroid. For $\beta = 16$, for example, this gives $r_{\rm min} = 7.8 \times 10^{-14+3\alpha}$ AU, which implies an asteroid of size 5 km ($\alpha = 2$) would have to pass by GAIA at a distance closer than 7.8×10^{-8} AU ≈ 10 km to generate an effect at a level of $10^{-\beta} = 10^{-16}$. Within the life span of GAIA ($\sim$5–10 yr), such close encounters (with such large objects) are highly unlikely in the neighborhood of the Earth/L2, and we therefore conclude we can safely neglect the contribution of individual (near-Earth) asteroids to gravitational time dilation at L2. Despite this conclusion, Fukushima (1995) argues that the 300 most massive asteroids (which have a cumulative mass of $\sim 10^{-9}$ M$_\odot$; Fukushima's Table 14) do influence the time ephemeris of the Earth at the level of $L_{\rm C} \sim 4.5 \times 10^{-18}$, and thus can influence, more generally, the outcome of the relativistic time-dilation integral for an arbitrary body in the Solar system (cf. Standish & Fienga 2002).

Figure 3 shows the time evolution of that part of the integrand of the relativistic time-dilation integral that corresponds to gravitational time dilation, i.e., $c^{-2}U_{\rm G}(t)$, split into the individual contributions of the

Table 1: Order-of-magnitude estimates of gravitational time dilation caused by Solar system bodies for an observer at L2. Columns: (1) name of the body; (2) orbital semi-major axis a (in AU); (3) mass M (in kg); (4–5) expected contribution to the gravitational time dilation at L2, $U_{\rm G}c^{-2} = GMr^{-1}c^{-2}$, for the extreme cases $r = |a - a_{\rm L2}|$ (providing a maximum value of $U_{\rm G}c^{-2}$) and $r = |a + a_{\rm L2}|$ (providing a minimum value of $U_{\rm G}c^{-2}$), where $a_{\rm L2} = 1.010\,078\,240\,44$ AU (Mignard 2002). For the Sun, the Earth, and the Moon, we only calculated the mean value of $U_{\rm G}c^{-2}$, i.e., for $r = |a - a_{\rm L2}|$. Column (6) shows, for the planets, the synodic period $P_{\rm syn}$ w.r.t. the Earth in units of days (Evans 2000). Column (7) shows, for comparison with columns (4–5), the (logarithm of the) mean gravitational force $F_{\rm G}$ (in Newton) exerted by the bodies on a test particle located at L2: $F_{\rm G} = GM\overline{r}^{-2}$ with $\overline{r} = (|a - a_{\rm L2}| + |a + a_{\rm L2}|)/2$. Data in the first 3 columns come from Weissman et al. (1999) and Arnett (2001). The moons of all planets are assumed to have identical orbital semi-major axes as their mother planets; the Moon's semi-major axis was chosen, in the context of this document, as 1 AU.

Name	a	M	$^{10}\log(U_{\rm G}c^{-2})$		$P_{\rm syn}$	$^{10}\log(F_{\rm G})$
	AU	kg	min	max	d	N
(1)	(2)	(3)	(4)	(5)	(6)	(7)
Sun	–	1.989×10^{30}	−8.01	–	–	8.94
Mercury	0.38710	3.302×10^{23}	−14.58	−14.93	115.88	2.16
Venus	0.72333	4.868×10^{24}	−13.07	−13.86	583.92	3.33
Earth	1.00000	5.974×10^{24}	−11.53	–	–	7.42
Moon (E1)	1.00000	7.350×10^{22}	−13.44	–		5.51
Mars	1.52366	6.418×10^{23}	−14.21	−14.90	779.94	2.09
1 Ceres	2.76675	8.700×10^{20}	−17.61	−17.94	–	−1.30
Jupiter	5.20336	1.899×10^{27}	−11.65	−11.82	398.88	4.50
Io (J1)	5.20336	8.930×10^{22}	−15.98	−16.15		0.17
Europa (J2)	5.20336	4.800×10^{22}	−16.25	−16.42		−0.10
Ganymede (J3)	5.20336	1.480×10^{23}	−15.76	−15.93		0.39
Callisto (J4)	5.20336	1.080×10^{23}	−15.89	−16.06		0.25
Saturn	9.53707	5.685×10^{26}	−12.48	−12.57	378.09	3.45
Dione (S4)	9.53707	1.050×10^{21}	−18.21	−18.31		−2.29
Rhea (S5)	9.53707	2.310×10^{21}	−17.87	−17.96		−1.95
Titan (S6)	9.53707	1.350×10^{23}	−16.10	−16.20		−0.18
Iapetus (S8)	9.53707	1.590×10^{21}	−18.03	−18.13		−2.11
Uranus	19.19130	8.683×10^{25}	−13.63	−13.67	369.66	2.02
Ariel (U1)	19.19130	1.350×10^{21}	−18.43	−18.48		−2.79
Umbriel (U2)	19.19130	1.170×10^{21}	−18.50	−18.54		−2.85
Titiana (U3)	19.19130	3.530×10^{21}	−18.02	−18.06		−2.37
Oberon (U4)	19.19130	3.010×10^{21}	−18.09	−18.13		−2.44
Neptune	30.06900	1.024×10^{26}	−13.76	−13.79	367.48	1.70
Triton (N1)	30.06900	2.150×10^{22}	−17.44	−17.46		−1.97
Pluto	39.48170	1.320×10^{22}	−17.77	−17.79	366.73	−2.42
Charon (P1)	39.48170	1.900×10^{21}	−18.61	−18.63		−3.26

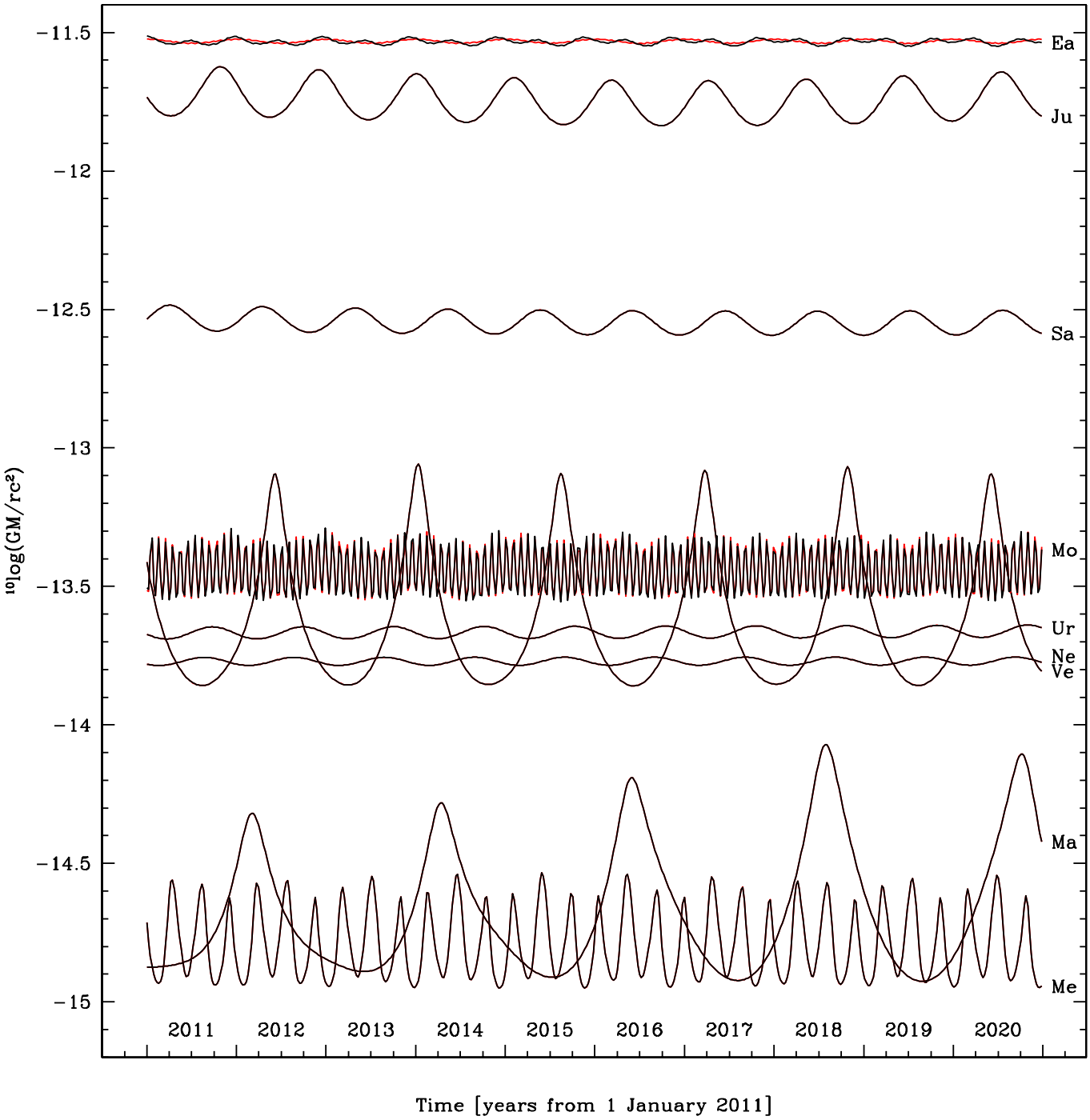

Figure 3: Black curves: the contribution of bodies in the Solar system to $c^{-2}U_{\rm G}(t)$ at the location of GAIA (§4.2), sampled at 7-day time steps over a 10-year interval starting 1 January 2011. The Sun falls outside the plotted range at $c^{-2}U_{\rm G} \approx 10^{-8}$; other objects, such as, e.g., the Galilean moons of Jupiter and Pluto, contribute at a level smaller than 10^{-15} (Table 1). Red curves (mostly underlying the black curves): as the black curves, but for an observer located at L2.

relevant Solar system bodies, with the exception of the Sun (which is located at $c^{-2}U_{\rm G} \approx 10^{-8}$). Black curves correspond to the case in which GAIA's orbit around L2, as described in §4.1, is accounted for; red curves — which are mostly underlying the black curves — correspond to the (hypothetical) case in which GAIA is located precisely at L2. As expected, the addition of GAIA's orbit is most relevant for bodies close to L2, i.e., the Earth and the Moon. The curves corresponding to the different objects show a complex time-variable behaviour, resulting from the interplay of several factors: the mass of the object, its mean distance to L2/GAIA, the orbital eccentricity (and inclination), the (relative) variations of the object–L2/GAIA separation, and the synodic period of the object w.r.t. L2/GAIA (see column 6 in Table 1). The predicted ranges of $c^{-2}U_{\rm G}$ (columns 4–5 in Table 1) are in good agreement with the DE405 ephemerides data. We conclude from Figure 3 and Table 1 that, for an assumed clock stability of 6×10^{-13} over 6 h (i.e., 1.5×10^{-12} over 1 h; see §4.3 and GAIA–JdB–004), it will be sufficient to limit the analysis of gravitational time dilation in the context of GAIA to the influence of the Sun, the Earth, Jupiter, and Saturn. Contrary to kinematic time dilation (§4.1), GAIA's orbit around L2 should be taken into account in relation to gravitational time dilation.

The level at which certain bodies contribute to gravitational time dilation at/near L2 (or to the gravitational potential $U_{\rm G} = GMr^{-1}$ at/near L2) might look surprising at first sight. Notably the Moon's rank, coming in only after the Sun, the Earth, Jupiter, and Saturn (in order of decreasing importance), might seem too low intuitively. For comparison, column (7) in Table 1 lists the strength of the gravitational force, $F_{\rm G} = GMr^{-2}$, exerted by the bodies in the Solar system on a (massless) test particle at the location of L2. In order of decreasing significance, we now find the Sun, the Earth, the Moon, Jupiter, and Saturn, from which we can conclude, not surprisingly, that a clear distinction between gravitational force and gravitational potential must be made.

4.3 Implications for the GAIA on-board clock

It is shown in GAIA–JdB–004 that GAIA's master clock should preferably be stable at the level of 6×10^{-13} over 6 h (i.e., 1.5×10^{-12} over 1 h; note that the accuracy of the latest Earth ephemerides, JPL DE405/TE405, is 0.1 ns and 10^{-16} for its derivative — Irwin & Fukushima 1999). Given this number, an important issue in relation to the actual implementation of a 'clock correction' scheme in the GAIA data processing is the rate at which kinematic and gravitational time dilation vary. Figures 4 and 5 display these rates per 1-h time step over an interval of 1000 d. Notably Figure 5 shows complex patterns, which can be understood by "combining" the magnitude and periodicity of the individual contributions as displayed in Figure 3. As kinematic and gravitational time dilation combined can induce frequency variations in GAIA's clock up to 3×10^{-13} h^{-1} — a value which is roughly an order of magnitude smaller than GAIA's projected clock stability (GAIA–JdB–004) —, a 'clock correction' will have to be made at a frequency of $\sim$1 h. A detailed analysis of GAIA's clock accuracy and stability requirements as well as details on the proposed 'clock correction' scheme are presented in GAIA–JdB–004.

Acknowledgements

I would like to thank Michael Perryman and François Mignard for helpful discussions.

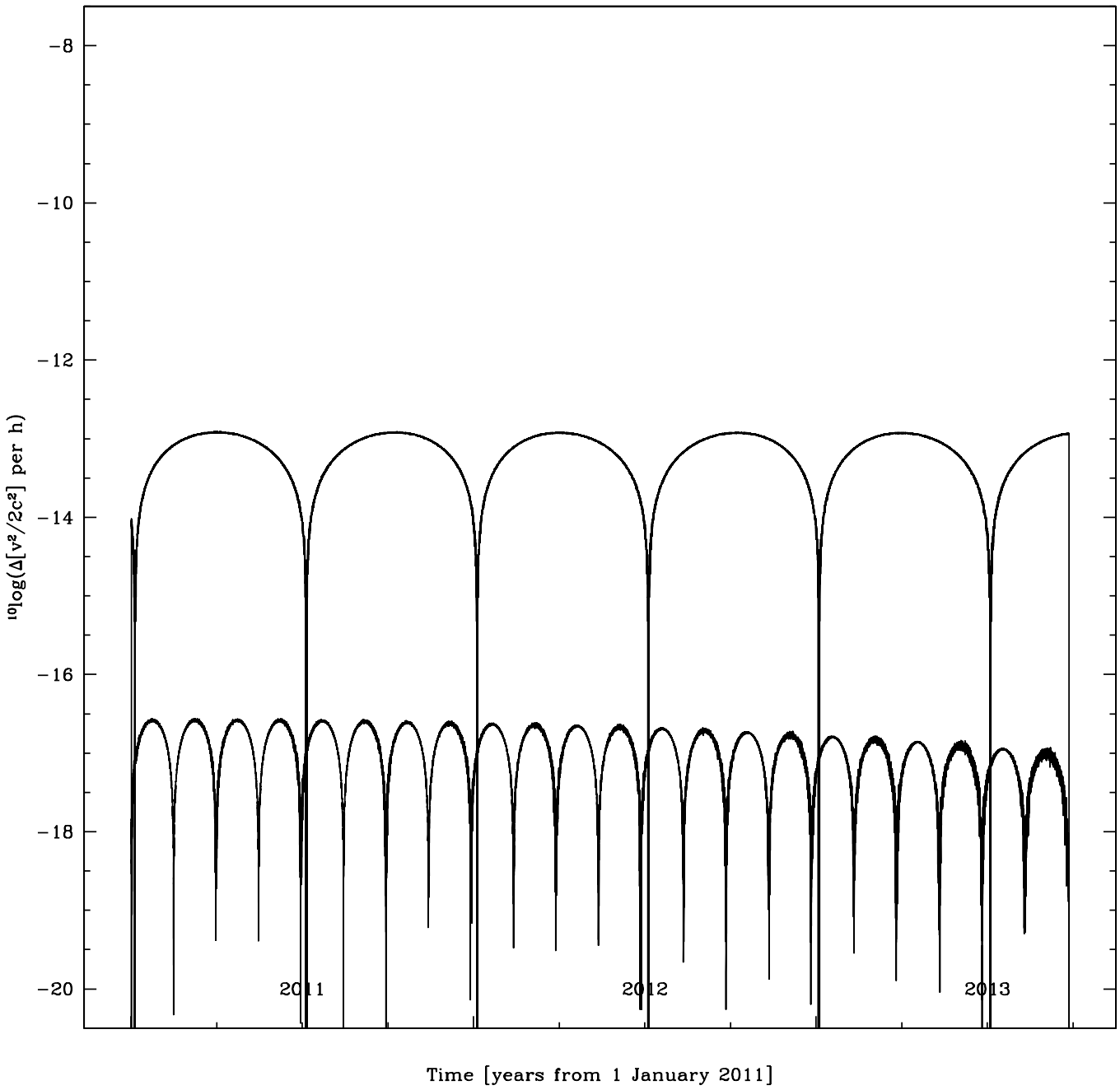

Figure 4: As Figure 2, but showing the rate at which kinematic time dilation varies per h (the time sampling is changed w.r.t. Figure 2 to cover a 1000-day interval in 1-h steps).

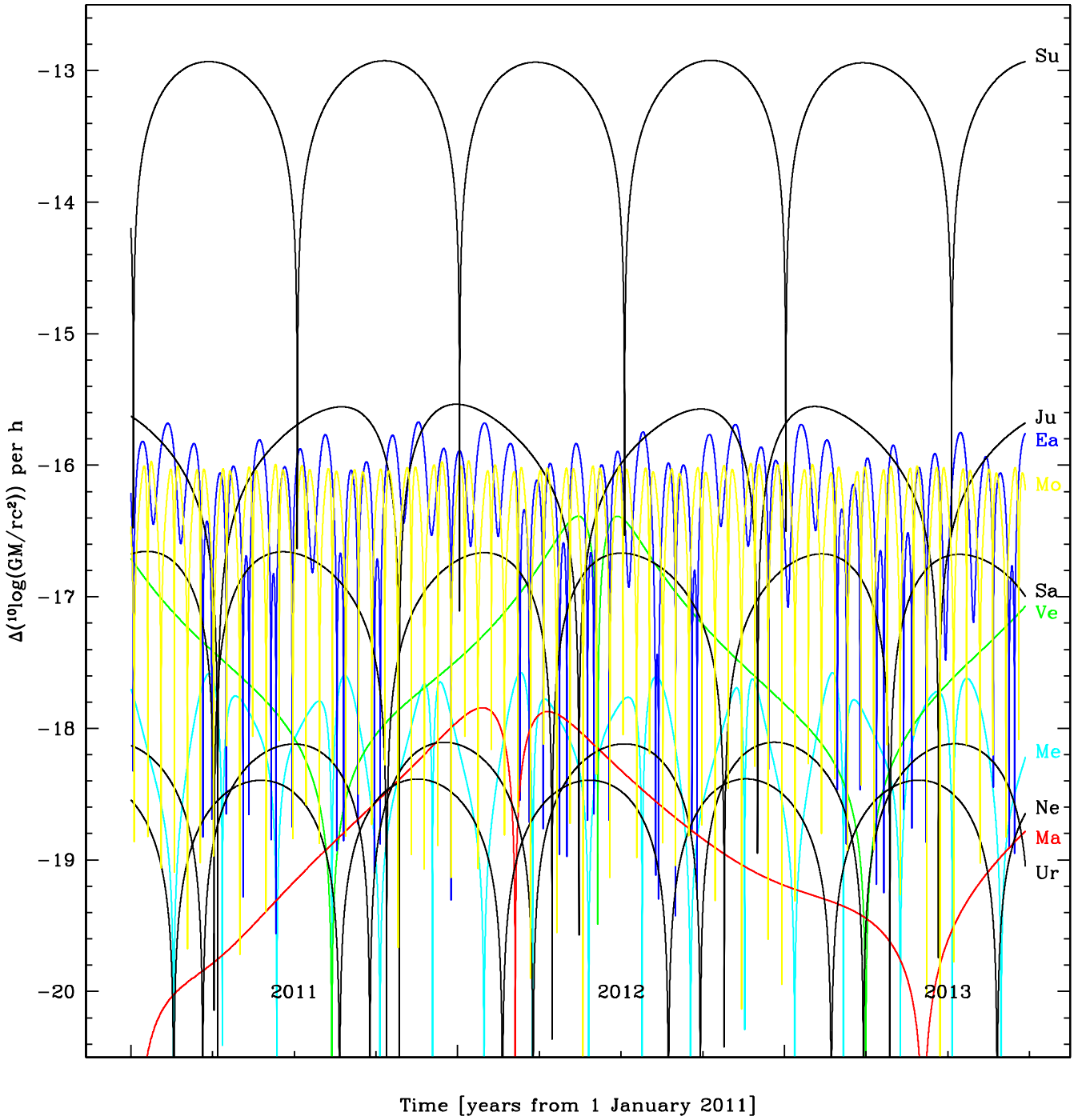

Figure 5: As Figure 3, but showing the rate at which gravitational time dilation varies per h (the time sampling is changed w.r.t. Figure 3 to cover a 1000-day interval in 1-h steps).

References

Arnett, B., 2001, http://www.seds.org/nineplanets/nineplanets/asteroids.html and data1.html

de Bruijne J.H.J., 2002, GAIA–JdB–001 "Gravitational light deflection"

de Bruijne J.H.J., 2002, GAIA–JdB–002 "Visualization of orbits of Near-Earth Objects"

de Bruijne J.H.J., 2003, GAIA–JdB–004 'GAIA clock accuracy and stability'"

Brumberg V.A., Groten E., 2001, A&A, 367, 1070

ESA, 1997, The Hipparcos and Tycho Catalogues (§1.2.3)

ESA, 2000, GAIA Concept and Technology Study Report, ESA–SCI(2000)4

Evans S.W., 2000, "Natural environment near the Sun/Earth–Moon L2 libration point", NASA MSFC (document available in Livelink; see also: http://208.183.181.52/space/ngst.gsfc.nasa.gov/doclist/bytitle.html http://www.ngst.nasa.gov/public/unconfigured/doc_0761/rev_01/index.html http://ngst.gsfc.nasa.gov/public/unconfigured/doc_0761/rev_01/NGST.pdf)

Fukushima T., 1995, A&A, 294, 895

Huang T.–Y., Han C.–H., Yi Z.–H., Xu B.–X., 1995, A&A, 298, 629

Klioner S.A., 2002, AJ, in press (astro-ph/0107457)

Mignard F., 1998, GAIA–FM–004 "Ephemeris requirements for GAIA"

Mignard F., 2002, GAIA–FM–011 "Considerations on the orbit of GAIA for simulations"

Pellón Bailón J.L., 2002, Technical Note "GAIA ranging" (document available in Livelink)

Petit G., 2002, "Coordinate times and time transformations: applying the IAU–1991 + IAU–2000 conventions to space geodesy techniques" (http://www.iers.org/workshop_2002/Session_41_Petit.pdf; cf. http://www.iers.org/)

Press W.H., et al., 1992, "Numerical recipes in Fortran", 2nd ed. (Cambridge Univ. Press)

Seidelmann P.K., 1992, "Explanatory supplement to the Astronomical Almanac" (Univ. Science Books)

Seidelmann P.K., Fukushima T., 1992, A&A, 265, 833

Shapiro I.I., 1964, Phys. Rev. Lett., 13, 789

Standish E.M., 1998a, A&A, 336, 381

Standish E.M., 1998b, JPL–IOM–312.F–98–048

Standish E.M., Fienga A., 2002, A&A, 384, 322

Thomas J.B., 1975, AJ, 80, 405

Weissman, P., McFadden, L., Johnson, T., 1999, *Encyclopedia of the Solar system* (Academic Press, San Diego) (We only had access to a restricted on-line version at http://www.academicpress.com/solar/Contents/chap1_2.htm)

Appendix A: GAIA's orbit

We will assume that $\mathbf{x}_{\rm L2}(t)$, i.e., the "orbit" of L2 relative to the Solar system barycenter, is available (see Appendix B for details), and that its spatial coordinates are $(X_{\rm L2}, Y_{\rm L2}, Z_{\rm L2})(t)$, where t denotes CT (i.e., $T_{\rm JPL}$; see Appendix B for the definition of the barycentric ecliptic XYZ-frame).

GAIA will perform its observations from a quasi-periodic Lissajous-type orbit around L2, the second Lagrange point of the Sun/Earth–Moon system. Mignard (2002) presents an analytic analysis of the restricted 3-body problem (involving the Sun, a fictitious body with the combined mass of the Earth and the Moon located at the Earth–Moon barycenter, and a massless satellite orbiting L2) and shows that an analytic prescription for GAIA's orbit around L2, adequate and relevant for simulations, is given by (see his equation 87; Figure 6):

$$\begin{aligned} \alpha(\tau) &= -\ 35\,000\cos(2\pi\sigma\tau); \\ \beta(\tau) &= \quad 110\,000\sin(2\pi\sigma\tau); \\ \gamma(\tau) &= \quad 110\,000\sin(2\pi\omega\tau), \end{aligned} \tag{13}$$

where τ is expressed in sidereal years (1 sidereal year = 365.256 36 d), $\sigma = 2.057\,014\,191$ per sidereal year, and $\omega = 1.985\,074\,856$ per sidereal year (see equations 52 and 40 in Mignard 2002). The coordinates (α, β, γ) in the above relations (expressed in units of km) are centered on L2 and are defined in a rotating frame (note that Mignard uses the symbols (X, Y, Z) for (α, β, γ)). The orientation of (α, β, γ) is such that, at any instant of time, α points outwards from the Sun (through the Sun/Earth–Moon barycenter and the Earth–Moon barycenter) to L2; β and γ complete the right-handed triad such that β lies in the ecliptic XY-plane and γ points up, at right angles, to this plane. The origin of time can be chosen freely here, as we are not concerned with eclipse avoidance features of the orbit (cf. Mignard 2002).

In order to be able to use equation (13) in the context of this investigation, we need to generalize the results of the restricted 3-body problem to the real Solar system. In particular, we need to reconsider (1) the definition of time τ in terms of CT (i.e., $T_{\rm JPL}$) and (2) the definition of the (α, β, γ) system in terms of the barycentric ecliptic XYZ-system (Appendix B).

1. Although Mignard derived equation (13) with time expressed in sidereal years, we take the liberty to interpret time as JPL ephemeris time CT (i.e., $\tau \longrightarrow T_{\rm JPL}$). In practice, this choice will affect the satellite's velocity, but at an insignificant level in the context of this investigation.

2. Contrary to the case of the restricted 3-body problem, the Sun, the Solar system barycenter, the Earth–Moon barycenter, and L2 are not strictly aligned, or even in a single plane, in reality. In the following, we redefine (α, β, γ) such that, at any instant of time, α points outwards from the Sun through L2; γ is chosen to lie, at right angles to α, in the plane defined by the α- and Z-axes; and β completes the right-handed triad (β will, by this definition, point parallel to the ecliptic XY-plane):

$$\begin{aligned} X_{\rm G}(t) = X_{\rm L2}(t) &+ \alpha(t)\cos\theta\cos\phi - \beta(t)\sin\phi - \gamma(t)\sin\theta\cos\phi; \\ Y_{\rm G}(t) = Y_{\rm L2}(t) &+ \alpha(t)\cos\theta\sin\phi + \beta(t)\cos\phi - \gamma(t)\sin\theta\sin\phi; \\ Z_{\rm G}(t) = Z_{\rm L2}(t) &+ \alpha(t)\sin\theta \qquad\qquad\qquad + \gamma(t)\cos\theta, \end{aligned} \tag{14}$$

   where

$$\begin{aligned} \phi = \phi(t) &= \mathrm{atan}\left(\frac{Y_{\rm L2} - Y_\odot}{X_{\rm L2} - X_\odot}\right); \\ \theta = \theta(t) &= \mathrm{atan}\left(\frac{Z_{\rm L2} - Z_\odot}{\sqrt{[X_{\rm L2} - X_\odot]^2 + [Y_{\rm L2} - Y_\odot]^2}}\right). \end{aligned} \tag{15}$$

   $(X_\odot, Y_\odot, Z_\odot)$ refer to the barycentric ecliptic Cartesian coordinates of the Sun. Figure 7 shows the orbit of GAIA corresponding to Figure 6 in the non-rotating frame $(X_{\rm G} - X_{\rm L2}, Y_{\rm G} - Y_{\rm L2}, Z_{\rm G} - Z_{\rm L2})$.

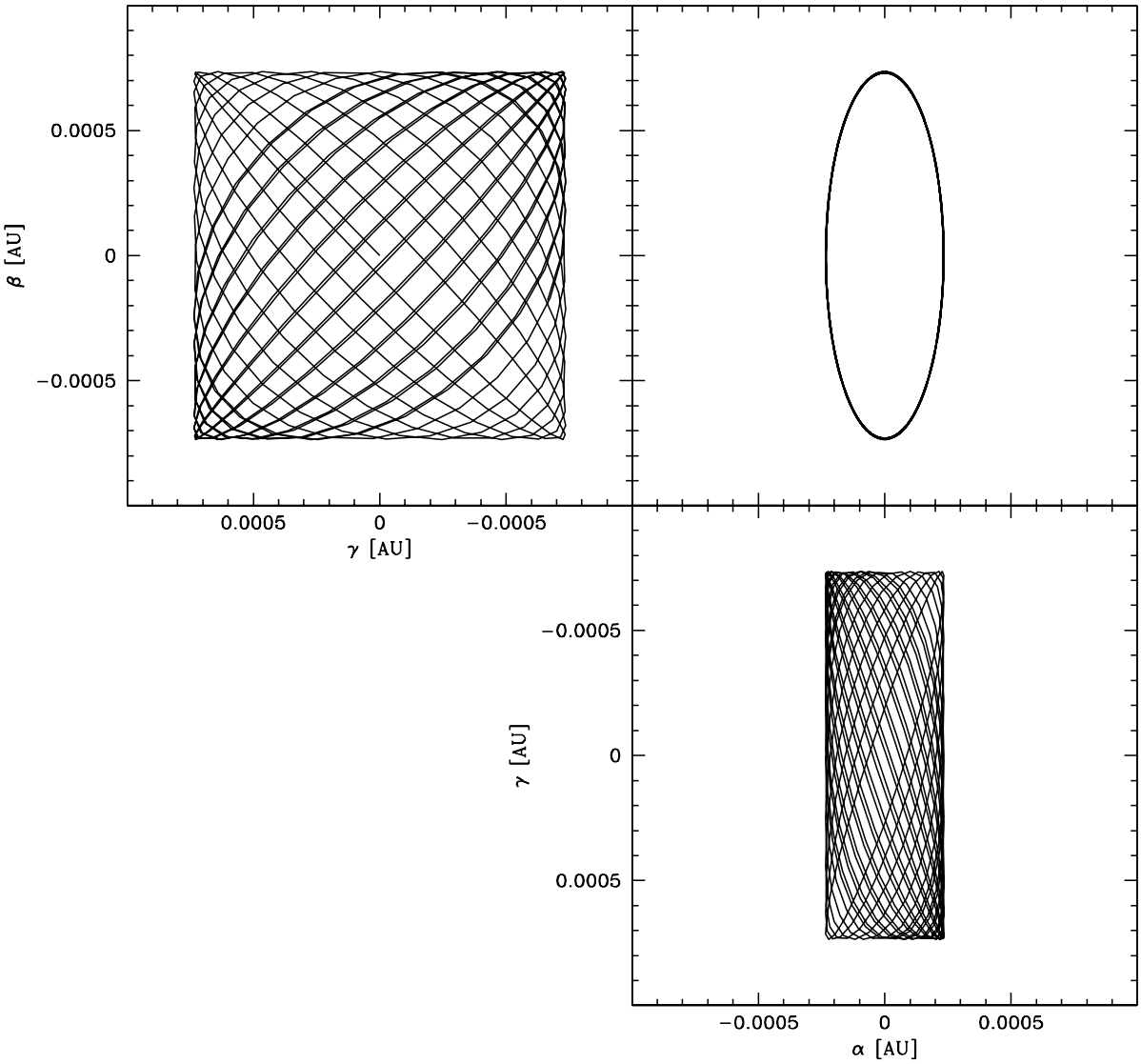

Figure 6: GAIA's orbit around L2, in a rotating frame, according to equation (13). Motion is shown over a 10-year interval in time steps of 7 days.

Appendix B: The JPL DE405 Planetary and Lunar ephemerides

JPL DE405 (Standish 1998b) is the latest Planetary and Lunar ephemerides available; it was created in May–June 1997. JPL DE405 spans the time interval JD 2305424.50 TDT (9 December 1599) to JD 2525008.50 TDT (20 February 2201) and is based upon the VLBI-based International Celestial Reference Frame (ICRF). Relativistic effects (expressed through order c^{-2}) are included in all planet, Lunar, and small-body dynamics, excluding satellites. DE405 can be accessed using four interfaces:

1. a Fortran program which reads the Spacecraft and Planetary Kernel SPK binary file `de405.bsp`;
2. the WWW (`http://horizons.jpl.nasa.gov/`);
3. telnet (`ssd.jpl.nasa.gov:6775`); and
4. email (`horizons@ssd.jpl.nasa.gov`).

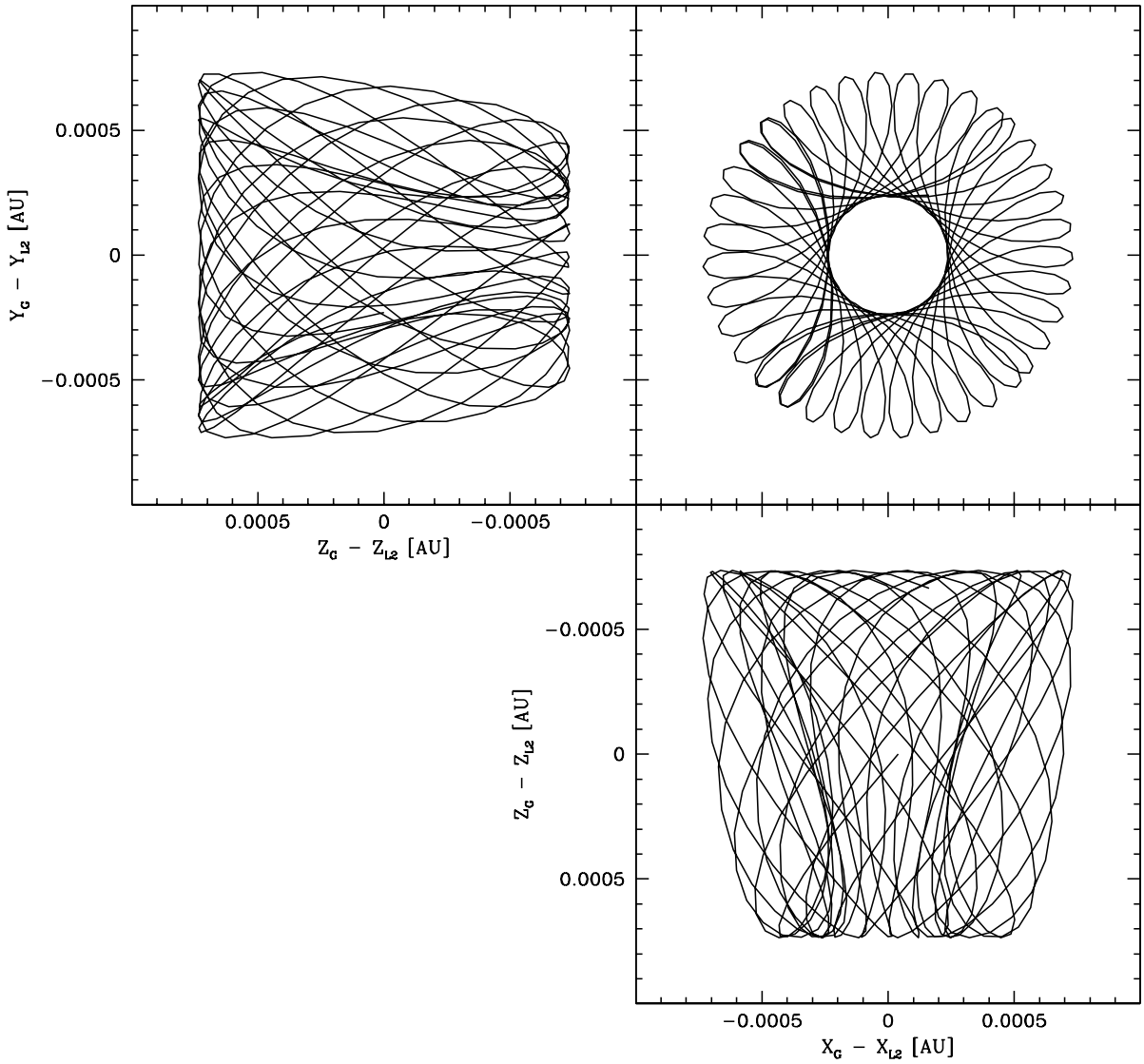

Figure 7: GAIA's orbit around L2, in a non-rotating frame, according to equation (14). Motion is shown over a 10-year interval in time steps of 7 days. See also Figure 6.

Whereas the WWW interface provides a restricted service only, options 3 and 4 offer a wide range of services (e.g., Cartesian vector and osculating element ephemerides, integration of user-defined orbits, and ephemerides for sites on bodies other than the Earth). Option 1 is equivalent to option 4 and has been considered in some detail in Appendix B of GAIA–JdB–002.

In this technical note, we are interested in obtaining the barycentric ecliptic Cartesian state vectors (X, Y, Z) (and associated velocities V_X, V_Y, V_Z) of the Sun, the planets, the Moon, and the second Lagrange point of the Sun/Earth–Moon system (L2). The XYZ-system is oriented as follows: the XY-plane is the plane of the Earth's orbit at the reference epoch J2000.0 (JD 2451545.0 TDB); the X-axis points out along the ascending node of the instantaneous plane of the Earth's orbit and the Earth's mean equator at the reference epoch J2000.0 ("mean" indicating that nutation effects are ignored in the frame definition); the Z-axis goes out perpendicular to the XY-plane in the directional sense of the Earth's north pole at the reference epoch J2000.0. $(X, Y, Z) = (0, 0, 0)$ denotes the Solar system barycenter, i.e., the spatial origin of the BCRS. The time coordinate associated with the spatial triad (X, Y, Z) is coordinate time (CT). CT is

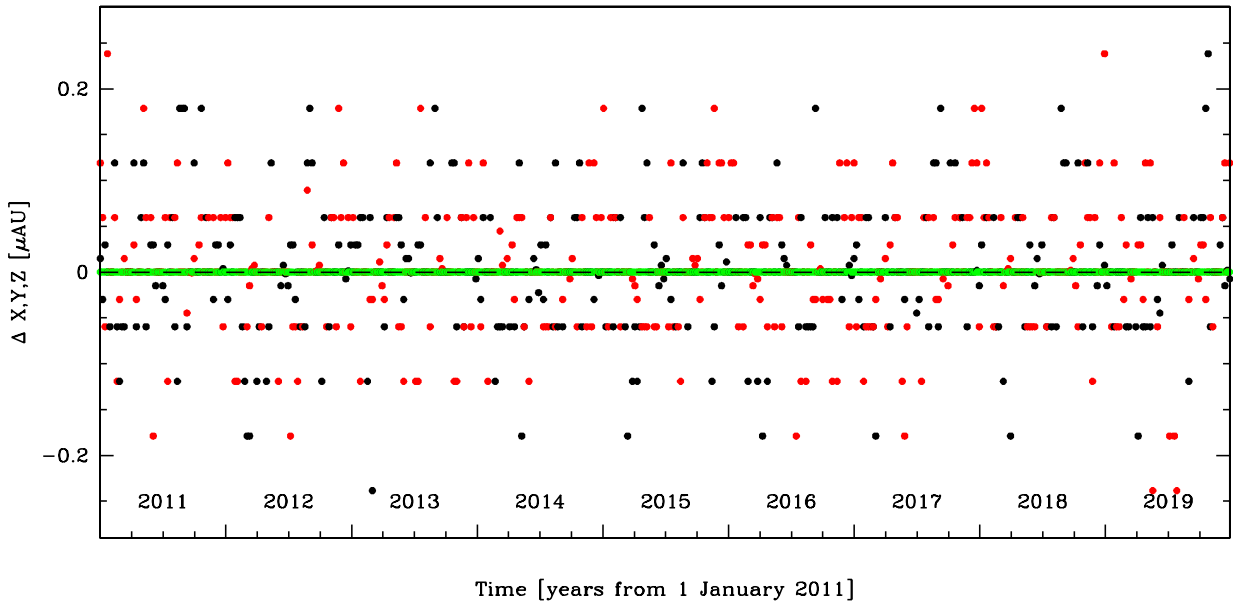

Figure 8: The black/red/green dots show the difference between "Mignard's (2002) prescription for the orbit of L2" and the JPL Cartesian ephemeris of L2 for the X, Y, Z spatial components, respectively, in units of micro-AU (μAU). The time interval is 1 January 2011 through 26 December 2019; the time step is 7 days.

the uniform time scale and independent variable of the JPL ephemerides (e.g., Standish 1998a). Formally, i.e., in a general-relativistic context, $(c \cdot \mathrm{CT}, X, Y, Z)$ is a four-vector in the BCRS (cf. §3.1).

Options 1 and 4 — the SPK and email interfaces to the JPL ephemerides — are the most suitable instruments for obtaining Cartesian state vectors for Solar system bodies. Email-requested Cartesian states are, following our choice (see below), returned in units of AU (coordinates) and AU day^{-1} (velocities), where 1 Julian day contains 86 400 s (in TDB), 1 Julian year contains 365.25 Julian days (in TDB), and 1 AU $= 1.495\,978\,706\,91 \times 10^{11}$ m (in TDB). The following sample email message (to be sent to `horizons@ssd.jpl.nasa.gov`) retrieves the Cartesian state vectors (X, Y, Z) and associated velocities (V_X, V_Y, V_Z) (in units of AU and AU day^{-1}, respectively) for the barycenters of Mercury (object 1), Venus (2), the Earth (3), Mars (4), Jupiter (5), Saturn (6), Uranus (7), Neptune (8), Pluto (9), the Sun (10), the Moon (301), and the L2 Lagrange point of the Sun/Earth–Moon system (392), all with respect to the Solar system barycenter ("500 @ 000"), from JD 2455562.50 (1 January 2011 00:00:00 CT) to JD 2457387.50 (31 December 2015 00:00:00 CT) in time steps of 1 day:

```
!$$SOF (ssd) JPL/Horizons Execution Control VARLIST
!
!            Send this email to: horizons@ssd.jpl.nasa.gov
!            The message SUBJECT line must contain the word "JOB"
!
EMAIL_ADDR = 'Jos.de.Bruijne@rssd.esa.int'
COMMAND    = '1','2','3','4','5','6','7','8','9','10','301','392'
OBJ_DATA   = 'YES'
MAKE_EPHEM = 'YES'
TABLE_TYPE = 'VECTORS'
CENTER     = '500 @ 000'
REF_PLANE  = 'ECLIPTIC'
START_TIME = 'JD 2455562.5'
```

```
STOP_TIME  = 'JD 2457387.5'
STEP_SIZE  = '1 days'
QUANTITIES = 'A'
REF_SYSTEM = 'J2000'
OUT_UNITS  = 'AU-D'
VECT_TABLE = '3'
!
!$$EOF+++++++++++++++++++++++++++++++++++++++++++++++++++++++++
```

L2's Cartesian coordinates are available only through 2019 and exclusively through the email interface. We therefore assume, following Mignard's (2002) analysis, that, at each instant of time, L2 sits a constant factor $1 + \rho$ (where $\rho = 0.010\,078\,240\,44$; see Mignard's equation 23) further from the Sun than the Earth–Moon barycenter (EMBC):

$$\begin{aligned} X_{\mathrm{L2}} = X_\odot &+ (1+\rho)\cdot(X_{\mathrm{EMBC}} - X_\odot) \\ Y_{\mathrm{L2}} = Y_\odot &+ (1+\rho)\cdot(Y_{\mathrm{EMBC}} - Y_\odot) \\ Z_{\mathrm{L2}} = Z_\odot &+ (1+\rho)\cdot(Z_{\mathrm{EMBC}} - Z_\odot), \end{aligned} \tag{16}$$

where $(X_\odot, Y_\odot, Z_\odot)$ denote the barycentric ecliptic Cartesian coordinates of the Sun. Figure 8 shows that this definition of L2 and JPL's ephemeris for L2 are consistent at the level of $\sim 2 \times 10^{-7}$ AU; this level of agreement is acceptable here.